PATTERNING AND MARKING OF TEXTURED AND UNTEXTURED SILICON SOLAR CELLS USING A 532 NM PICOSECOND FIBER LASER
M306

Tim D. Gerke[1], Brian Baird[2]

[1] Fianium Inc., 858 W. Park St., Eugene, OR 97401, USA
[2] Summit Photonics, 5829 Jean Road, Lake Oswego, OR 97035, USA

Abstract

Laser microprocessing is key to the development and manufacture of advanced silicon photovoltaics. In this paper a picosecond laser is used to pattern and mark the surface of both textured and non-textured passivated silicon photovoltaics as well as unpassivated silicon wafers. The laser is a master oscillator fiber power amplifier that provides 30 picosecond pulses at 532 nm with pulse energy up to 5 micro-Joules. We evaluate and compare techniques for marking and patterning crystalline-silicon substrates utilizing a conventional Gaussian beam and a flat-top spatially-shaped square beam. We show that SiO_2 and SiN passivation layers on both textured and non-textured crystalline-silicon photovoltaics can be removed in arbitrary patterns. We demonstrate that not only can the passivation layers be removed, but the surface of either passivated or unpassivated silicon substrates can be marked in a continuum of shades of gray and in arbitrary patterns. These results demonstrate the promising capability for advanced patterning and marking of photovoltaic devices and for marking of silicon wafers with picosecond fiber lasers.

Introduction

Ultrafast laser microprocessing is a rapidly growing field and encompasses applications such as photovoltaic processing [1], wafer dicing [2,3], and marking [4,5] to name a few. The ultrashort pulse durations on order of a few picoseconds or less provide an avenue to micromachining in an athermal regime that is inaccessible with longer pulsewidths [6] and important for a range of applications. One particular application that has very significant opportunity for growth is in laser marking. New requirements for Unique Device Identification (UDI) of certain medical devices is certain to add to the already growing market for laser marking. A vast array of materials can be marked with ultrafast lasers including silicon [7,8], silicon nitride films [9], glass [10], ceramic ICs [11], stainless steel [12], aluminum [13], as well as most other metals and many more materials in general.

In particular with ultrafast laser marking of silicon, investigation into the formation of black silicon has generated specific interests. Originally, extremely high quality nanostructures in the shape of sphere-topped cones (like a forest of pine trees each topped with small orbs) were demonstrated with the use of femtosecond laser pulses in an atmosphere of SF_6 [7]. Shortly thereafter similar results were reported using femtosecond laser pulses in vacuum [8], but in this second instance the nanostructures were less uniform and resembled a congregation of penguins rather than a pine forest. The less uniform nanostructures enhanced absorption nearly as well as the higher-quality structures (91% versus 94% absorption) despite the obvious structural difference.

For this paper we first demonstrate the ability to selectively remove SiN and SiO_2 dielectric passivation and AR coatings from both textured c-Si PV wafers using a picosecond fiber laser made by Fianium Ltd. This effort is a significant extension of our previous reporting, which demonstrated removal of SiN from c-Si wafers [9]. We demonstrate here not only the ability to remove the dielectric layers, but also to mark the underlying silicon in grayscale by tailoring the laser parameters, including pulse overlap, processing speed, and fluence. Our black areas are similar to previous reports on fabrication of black silicon generated by femtosecond lasers. The results show a simple and cost effective avenue to marking and patterning textured and untextured silicon wafers through the use of a robust picosecond fiber laser.

Picosecond Laser

The laser source employed in this work is the Fianium HE1060/532 picosecond fiber master oscillator power amplifier (MOPA). It is capable of providing either 1064 nm or 532 nm output via dual electronically selectable output ports. The laser comprises a low power passively modelocked fiber master oscillator which seeds a high gain, single mode cascaded fiber amplifier. The laser system also comprises modulation capability, enabling selection of pulse repetition rate from single-shot to 20 MHz, with maximum pulse energy attainable at repetition rates up to 1 MHz.

The Fianium picosecond fiber laser used for the experimental work in this paper provides a maximum energy per pulse at 200 KHz for the 1064 nm output of 10 μJ and 5 μJ for the 532 nm output. The laser beam profile is Gaussian and the M^2 has been measured to be less than 1.2. A typical beam profile obtained using an Ophir-Spiricon camera system is shown in Figure 1. The laser includes a power supply and integrated air-cooling system with a fiber-coupled remote head that enables simple customization and integration of the laser within laser processing systems.

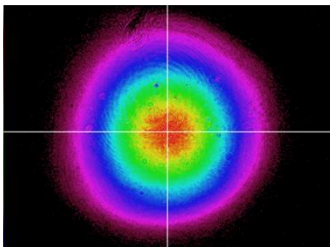

Figure 1. 2D beam profile of the Fianium HE1064/532 picosecond fiber laser.

Fabrication System

The laser output is directed through a 2-8x variable beam expander that provides control of the spot size at the work surface from 10-60 μm. The expanded beam is directed into a Scanlab Hurryscan II-14 galvanometric scanner with a 100 mm focal length telecentric objective lens. The galvo scanner can control the spot on the work surface with a resolution of a few micrometers and can scan at speeds of over 10 m/s. The ultrafast laser micromachining system is capable of fabricating arbitrary patterns with feature sizes down to under 10 μm. The substrates are placed upon a 2D translation stage that is mainly used to locate the illumination focus. All the equipment was computer-controlled for synchronous control of the laser output and the spot location on the work surface.

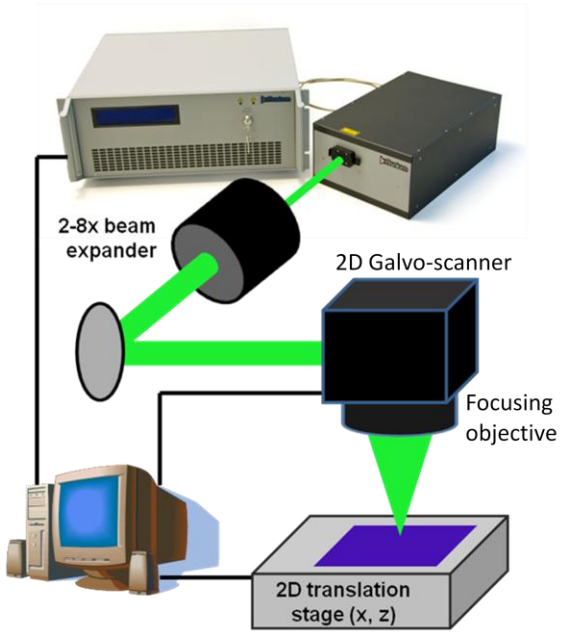

Figure 2. Ultrafast laser micromachining system. Picosecond pulses from Fianium's ultrafast fiber laser are directed through a 2-8x beam expander and into a 2D galvanometric scanner system that controls the focused spot location on the work surface.

Experimental Results

SiN and SiO_2 Removal

The Fianium 532 nm picosecond fiber laser and the processing system outlined in the previous section are used to selectively remove SiN and SiO_2 from c-Si wafers. The dielectric layers can be removed and patterned from both the untextured and textured silicon wafer with single laser pulses. Dielectric layers are conventionally removed using more costly and cumbersome UV lasers for direct absorption in the dielectric. A lift-off approach, however, provides the capability of a 532 or 1064 nm laser to remove the dielectric without any direct absorption in that layer. Instead the physical process involves a very thin layer of the underlying silicon absorbing the laser energy, vaporizing, and ejecting the above dielectric material. The amount of silicon ablated is small enough (<100 nm) that it is unlikely to significantly affect the device performance, particularly for applications such as emitter wrap-through or metal wrap-through where the removal is followed by a metal contact deposition over the cleared area.

Textured silicon has enhanced absorption, and enhanced efficiency, over polished silicon and is hence becoming a preferred technology. Removal of the dielectric AR/passivation layer from textured silicon

wafers, however, has historically proven to be more difficult and often significant remnants of the dielectric are left behind [14]. Figure 3 shows two picosecond laser scribes of SiN on untextured and textured wafers alike, and demonstrates complete removal of the dielectric layer from both substrates. In the top figure (untextured Si) some artifacts appear in the pulse overlap regions, which under SEM were determined to be small amounts of melted Si that were pushed aside and do not contain measureable quantities of the dielectric SiN coating.

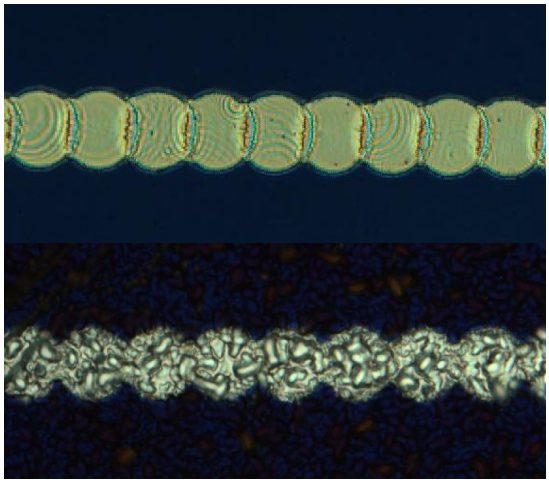

Figure 3. Scribes of SiN on untextured (top) and textured (bottom) silicon wafers.

Given the computer-controlled direct-write nature, the process is not limited to linear scribes but is capable of removing the dielectric layer in large areas and arbitrary patterns. In fact an area of SiN 2x0.5 mm was removed at a rate of approximately 10 mm^2/s and is shown in Figure 4.

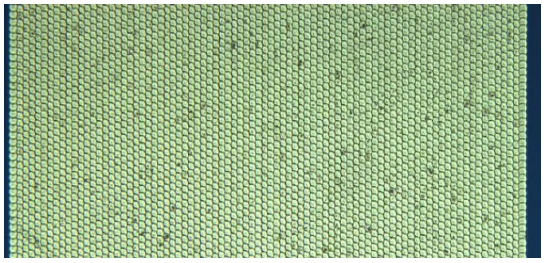

Figure 4. An area of SiN completely removed from the underlying silcon wafer. Each small circle denotes an area cleared by a single laser pulse.

The single-pulse removal of the dielectric layer that we have demonstrated above and previously [9] is a useful technique for advanced cell technologies such as emitter wrap-through and metal wrap-through. In these embodiments small areas of the AR/passivation coatings must be removed from the front face of the wafers for forming contact areas.

We also used a flat-top square beam profile for clearing the dielectric passivation/AR coating. The square beam was generated using a HoloOr refractive/diffractive hybrid top hat beam shaper. The optic generates a 100 μm square beam profile that was then imaged to the work surface by a collimating lens and the scanner objective focusing lens. The magnification factor of the lens pair resulted in a square approximately 40 μm on a side.

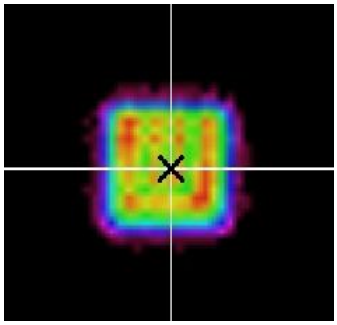

Figure 5. 2D beam profile of the square-shaped top hat beam.

The square shape is an improved geometry over a Gaussian beam because the profile edges are much more pronounced, which allows for material to be removed in a more selective fashion. The steep profile edges also help to minimize any occurrence of defects that are caused by insufficient energy for ablation like peeling, microcracks, and melting. Figure 6 shows SEM images of scribes of the SiN coating using (a) a flat-top square beam profile and (b) a Gaussian beam profile. The square beam scribe does appear to be improved over the Gaussian result in that there appears to be less melting occurring at the scribe edges. In addition the square profile results in straighter scribe edges and tiles more efficiently to remove large areas.

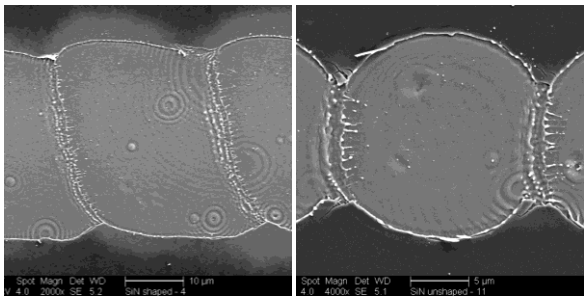

a. b.

Figure 6. SEM image of a scribe of the SiN coating on a c-Si substrate using (a) a flat-top square beam profile and (b) a Gaussian beam profile.

Silicon Wafer Marking

Another important application for laser processing of silicon PVs is marking for identification and quality control. For marking purposes simply removing the dielectric layer is insufficient and selective darkening is preferred. As discussed in the introduction, previous work involving femtosecond lasers in controlled atmospheres has been conducted to selectively darken polished silicon wafers [7,8]. The final results were capable of visible light absorption as high as 94%. The requirements for costly amplified femtosecond lasers and controlled atmosphere, however, are prohibitive to commercial application of the technique.

We demonstrate in Figure 7 the ability to either (a) remove the SiN layer and leave a semi-reflective surface or (b) to darken areas, both in arbitrary patterns and using a picosecond laser processing system in an open environment. The semi-reflective areas enhance reflection relative to the AR-coated region and the darkened areas significantly enhance the absorption relative to the AR coating. The images also prove the capability to create arbitrary patterns, such as 2D barcodes, company logos, or other markings using a simple, cost-effective, and maintenance-free picosecond fiber laser. The marks can be either micro or macro scale with a minimum feature size on order of 10 μm and a marking rate around 1-20 mm^2/s depending on the darkness desired.

a. b.

Figure 7. Two identical patterns made with different process parameters demonstrates the stark difference between (a) removal of the SiN layer and (b) marking/darkening the silicon beneath.

The goal of this work, however, is to demonstrate true gray-scale capability as a continuum of shades of reflection from 0 to 100% (relative to unpolished Si). The marks we made to investigate darkness were raster-scanned squares (see Figure 8) where the linear speed was variable as was the line to line separation. We attempted matrices of square marks where laser fluence was varied along one axis and either scribe speed or line separation was varied along the other. Scribe speed and line overlap were determined to function similarly; as scribe speed or line separation increased (both decreasing the total dosage) the darkness decreased, and vice versa. Figure 9 shows a picture of one of the arrays of squares made with varied process parameters. It demonstrates that in one corner where the total dosage was maximum (high fluence and slow speed or low line separation) the marks are darker, and in the opposite corner, the dosage was insufficient to have much effect. The rest of the squares demonstrate some varying degree of darkening.

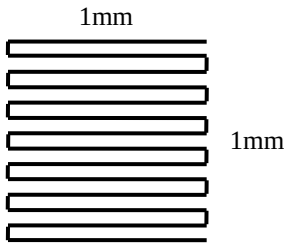

Figure 8. The scanning geometry used to mark squares on silicon wafers was a raster-scanned square.

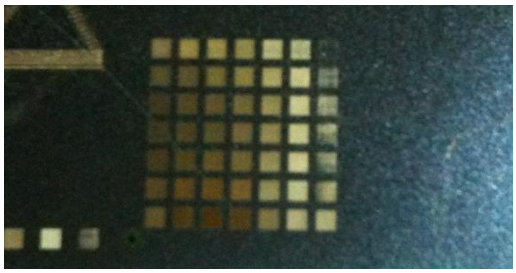

Figure 9. Picture of an array of marked squares on textured silicon with increasing process speed from bottom to top and decreasing laser fluence from left to right.

An interesting and surprising result can also be seen in Figure 9. The bottom row was made at the slowest writing speed and with decreasing fluence from left to right. The darkness of the mark actually appears to reach an optimum at a moderate fluence as opposed to becoming darker and darker with higher and higher fluence values (right to left). This surprising result was repeatable for both textured and untextured, and passivated and unpassivated silicon wafers. It demonstrates that process optimization is important for creating the darkest marks possible on silicon wafers.

For one particular trial on untextured passivated silicon, we captured images using a microscope to compare diffuse reflectivity. The microscope objective power was 20x and the camera had a fixed gain and exposure so that all the images could be directly compared. We focused on the silicon surface and captured images for each box from a trial similar to that shown in Figure 9. For this trial we varied fluence along the y-axis and linear scribe speed along the x-axis. The resulting images are tiled as they were physically laid out and can be seen in Figure 10. For the lowest fluence value, no significant modification was observed at the fastest four scribe speeds, and consequently no images were taken. The lines that can be seen in a few images were remnants of other processing trials that happened to overlap with a few of the marks and should be ignored. Many of the squares appear to be quite dark, which suggests that making dark marks is a relatively simple process to tailor with a relatively wide processing window. On the other hand, because only a few marks are at intermediate darkness shades, writing lighter shades of grayscale appears to be more difficult and exists within a more constrained and narrow process window. Regardless, the array demonstrates that many shades from very black to almost uncoated silicon reflectance are achievable.

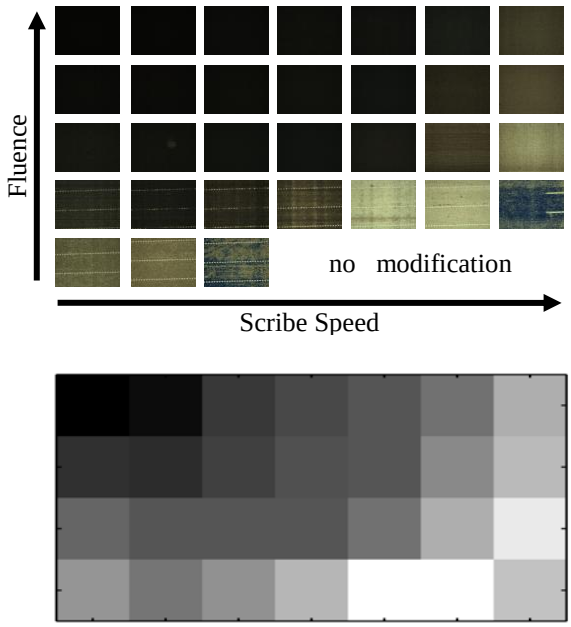

Figure 10. Array of marked squares on polished silicon with increasing fluence from bottom to top and increasing process speed from left to right. The lower image is the grayscale log-plot of the average intensity of each image, first four rows only.

We selected six particular marks and plotted their respective reflection values in Figure 11 and the values are also listed in Table 1. The marks were selected to best fill the continuum from as dark as possible to the highest reflection possible. The relative reflection values ranged from 3% to 100%, and we expect that with the correct process conditions any value in that range could be achieved. Reflection is reported relative to the highest reflection or brightness we measured, which was for the boxes that appear to be bare Si with the dielectric and AR coating removed and with minimal modification to the Si itself (row 4, col 5 in Figure 10). This value of brightness was found to be 19.6% relative to a polished aluminum mirror in the visible spectrum. Another useful frame of reference is the unmodified AR coating (similar to row 4, column 7 in Figure 10). We measured the AR coating reflection to be 2.4% relative to the mirror, or 12.2% relative to the cleared Si (row 4, col 5 in Figure 10).

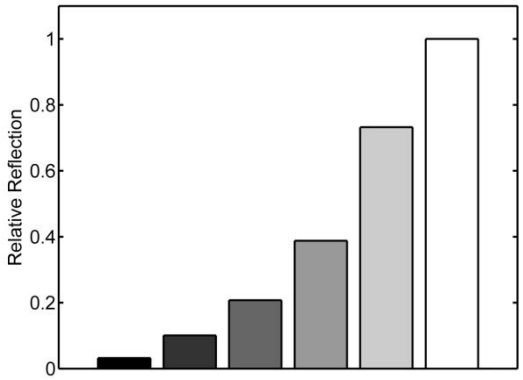

Figure 11. Relative reflection values for selected process results that demonstrate the capability for six discrete gray levels.

Table 1. Reflection values and process parameters for selected grayscale marks shown in Figure 10.

Relative reflection (%)	Fluence (J/cm^2)	Linear scribe speed (mm/s)
3.19	0.08469	50
10.08	0.05227	200
20.75	0.06308	1000
38.79	0.06308	2000
73.24	0.05227	2000
100.00	0.04146	500
42.2	AR coating	AR coating

A whole host of marks are realizable with this simple technique. Grayscale marks and arbitrary binary patterns with feature sizes down to only a few microns are possible. Figure 12 shows the Fianium company logo marked on a passivated polished silicon wafer and on a passivated textured silicon wafer. The polished image is of much higher quality because of its constant background. The textured silicon includes a highly irregular background that makes the lighter marks difficult to read well.

On the other hand, darker marks that we can also make employing our technique are somewhat easier to read on the textured silicon, as demonstrated in Figure 13b. Figure 13 shows dark marks made in the pattern of a 2D barcode on (a) untextured and (b) textured c-Si. Both marks are significantly darker than the AR coated surroundings and are easily readable, although the constant background of the untextured substrate creates a clearer image.

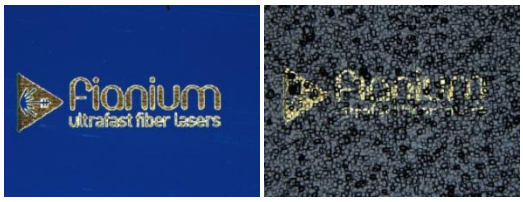

a b

Figure 12. Arbitrary marks, such as company logos can be written on both (a) polished and (b) textured silicon wafers.

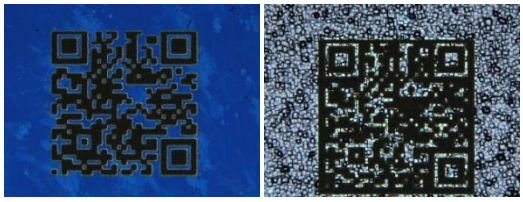

a b

Figure 13. Arbitrary marks can be written on both (a) polished wafers coated with SiN and (b) textured silicon wafers coated with SiO_2. The black marks are much more readable on the textured than lighter marks.

The flat-top square shaped beam was also used to mark the c-Si substrates. The results were similar to those achieved with Gaussian beam profile and thus were not further investigated and are not being further described here.

Conclusions

A Fianium picosecond fiber laser was used to selectively remove the SiN and SiO_2 dielectric AR/passivation coatings from textured and untextured c-Si PVs. Both a flat-top square beam profile and a conventional Gaussian beam profile were used to remove the dielectric layers. The shaped beam profile was observed to provide improved material removal, particularly in the edges of the scribes. Removal of the dielectric layers is important for advanced cell technologies like emitter-wrap through and metal-wrap through and can also be used for marking purposes. In addition, we used the picosecond laser to mark the underlying c-Si in shades of gray. The reflection of the resulting marks varied from 3-100% relative to the most reflective mark. The lowest reflection result was also close to the noise floor of the camera, which suggests the actual reflection may be even better than reported here. Finally, a number of shades of gray were also created by varying the laser fluence or the process speed. These results demonstrate that a picosecond fiber laser is a useful tool for selectively

marking textured and untextured passivated c-Si PV devices.

References

[1] Huber, H. P., Herrnberger, F., Kery, S., and Zoppel, S., (2008) Selective structuring of thin-film solar cells by ultrafast laser ablation, Proceedings of SPIE Commercial and Biomedical Applications of Ultrafast Lasers VIII 688, 688117.

[2] Kim, T., Kim, H.S., Hetterich, M., Jones, D., Girkin, J.M., Bente, E., and Dawson, M.D., (2001) Femtosecond laser machining of gallium nitride, Mater. Sci. Eng. B 82, 262.

[3] Gu, E., Jeon, C. W., Choi, H. W., Rice, G., Dawson, M. D., Illy, E. K. and Knowles, M. R. H., (2004) Micromachining and dicing of sapphire, gallium nitride and micro LED devices with UV copper vapour laser, Thin Solid Films 453-454, 462-466.

[4] Vorobyev, A. Y., and Guo, C., (2005) Enhanced absorptance of gold following multipulse femtosecond laser ablation, Phys. Rev. B 72, 195422.

[5] Vorobyev, A. Y., and Guo, C., (2007) Looking at femtosecond laser-induced black metals at different polarizations, Optics and Photonics News 18(12), 43.

[6] Corkum, P. B., Brunel, F., Sherman, N. K., and Srinivasan-Rao, T., (1988) Thermal response of metals to ultrashort-pulse laser excitation, Phys. Rev. Lett. 61, 2886-2889.

[7] Her, T.-H., Finlay, R. J., Wu, C., Deliwala, S., and Mazur, E., (1998) Microstructuring of silicon with femtosecond laser pulses, Appl. Phys. Lett. 73, 1673-1675.

[8] Sarnet, T., Halbwax, M., Torres, R., Delaporte, P., Sentis, M., Martinuzzi, S., Vervisch, V., Torregrosa, F., Etienne, H., Roux, L., and Bastide, S., (2008) Femtosecond laser for black silicon and photovoltaic cells, in Proceedings of SPIE Commercial and Biomedical Applications of Ultrafast Lasers VIII 688, 688119.

[9] Gerke, T. and Baird, B., (2010) Picosecond ablation of silicon nitride using 532 nm master oscillator fiber power amplifier for patterning crystalline photovoltaic, in Proceedings of ICALEO, Anaheim, California, USA, pp. 1-2.

[10] Hong, M. H., Sugioka, K., Lu, Y.F., Midorikawa, K., and Chong, T.C., (2002) Laser microfabrication of transparent hard materials and signal diagnostics, Appl. Surf. Sci. 186, 556-561.

[11] Noor, Y. M., Tam, S. C., Lim, L. E. N., and Jana, S., (1993) A review of the Nd: YAG laser marking of plastic and ceramic IC packages, J. Mater. Proccess. Tech. 42, 95-133.

[12] Dusser, B., Sagan, Z., Soder, H., Faure1, N., Colombier, J. P., Jourlin, M., and Audouard, E., (2009) Controlled nanostructrures formation by ultrafast laser pulses for color marking, Opt. Express 18, 2913-2924.

[13] Vorobyev, A. Y., and Guo, C., (2008) Colorizing metals with femtosecond laser pulses, Appl. Phys. Lett. 92, 041914.

[14] Rana, V., Zhang, Z., Lazik, C., Mishra, R., Weidman, T., Eberspacher, C., (2008) "Investigations into selective removal of silicon nitride using laser for crystalline silicon solar cells," 23rd European Photovoltaic Solar Energy Conference Proceedings, pp. 1942-1943.

Meet the Authors

Tim Gerke received his B.S. and M.S. degrees in Electrical and Computer Engineering from Purdue University in 2002 and 2004 respectively, and his Ph.D. in Electrical and Computer Engineering at the University of Colorado in 2011. He is currently the Laser Applications Engineer for Fianium Inc., a fiber laser company specializing in ultrafast fiber lasers. His academic research background includes diffractive optics, 3D ultrafast laser nano-machining, ultrafast material processing, and characterization and fabrication of nanophotonic devices.

Brian Baird received the B.S. degree in Physics from the University of Oregon in 1980, his M.S. in Physics from the University of Washington in 1984 and his Ph.D. in Applied Physics from the Oregon Graduate Institute of Science and Technology in 1997. He is the founder and Managing Director of Summit Photonics LLC, a photonics engineering services firm, specializing in solid state photonics and laser processing systems. From 1988 to 2008, he worked at Electro Scientific Industries where he contributed to the research and development of successive generations of laser processing systems. Dr. Baird currently holds fourteen patents.